CFD Study of Fire-Induced Pressure Variation in a Mechanically-Ventilated Air-Tight Compartment

Li J.Y.*, Beji T., Merci B.

Ghent University, Department of flow, heat and combustion mechanics,
Ghent, East Flanders Province, Belgium
**Corresponding author's email: Junyi.Li@UGent.be*

ABSTRACT

The present work describes Computational Fluid Dynamics (CFD) simulations of fire-induced pressure rise and ventilation duct flow rate in a mechanically-ventilated air-tight compartment, which represents a passive house. Overlapping wooden slats were used as fire source in the experiments and were represented in the simulations by a 0.4 m × 0.4 m × 0.4 m cube with a prescribed HRR based on the experimental results. The maximum ventilation volume flow rate was set to 80 m^3/h in the experiments, in line with Belgian requirements for residential ventilation. Two methods were used to set up the ventilation volume flow rate in the simulations to meet the requirement of maximum ventilation flow rate by modifying the fan curve, and adding dampers. As expected the combination of the real fan curve and dampers, which resembles reality better, is morein line with the experimental results. The maximum over-pressure in the fire room was about 420 Pa, resulting in a reverse flow in the supply duct and an enhanced flow in the exhaust duct. The reversed inlet volume flow rate and increased outlet volume flow rate reached 137 m^3/h and 175 m^3/h respectively. The fire-induced pressure is high enough to hinder evacuation and fire rescue operations due to the impossibility of opening inward-open doors over a certain period of time. Moreover, the pressure rise in the adjacent room also reaches a dangerous level. Reducing the gap area between rooms can significantly decrease the pressure rise in the adjacent room, but leads to an increase of pressure in the fire room. As expected, when applying mechanical ventilation, the influence of leakage pressure exponent on pressure rise is smaller compared to cases without ventilation.

KEYWORDS: CFD modeling, duct reverse flow, fire-induced pressure, passive house fire.

NOMENCLATURE

A	area (m^2)
c_p	specific heat of fluid (kJ/(kg·K))
D^*	characteristic length scale (m)
g	gravitational acceleration (m/s^2)
K	loss coefficient (-)
n	leakage pressure exponent (-)
Δp	pressure difference (Pa)
$\dot{Q}$	heat release rate (kW)
T_∞	ambient air temperature (K)
$\dot{V}$	volume flow rate (m^3/s)
Greek	
ρ_∞	ambient air density (kg/m^3)
Subscripts	
d	diaphragm
eff	effective
L	leakage
$minor$	minor losses
ref	reference

INTRODUCTION

With the increased energy-saving demand, air-tight passive houses are more and more used in architectural design. Passive houses can significantly reduce the total energy demand over the life cycle of the buildings [1]. Many passive strategies are applied to minimize the consumption of energy,

Proceedings of the Ninth International Seminar on Fire and Explosion Hazards (ISFEH9), pp. 574-583
Edited by Snegirev A., Liu N.A., Tamanini F., Bradley D., Molkov V., and Chaumeix N.
Published by St.Petersburg Polytechnic University Press
ISBN: 978-5-7422-6496-5 DOI: 10.18720/spbpu/2/k19-25

such as boundary insulation, heat recovery, passive house windows, airtightness and thermal bridge reduced design. The present paper will focus on the influence of airtightness on the pressure build-up during fires.

The airtightness indeed poses additional fire risks to such buildings. Due to the low leakage, the hot combustion products cannot easily escape from the enclosure, resulting in a high pressure rise. Cases have been reported where the fire-induced pressure reached a level preventing the occupants from opening the door and evacuating [2].

Some research results also demonstrated that the pressure variation in a passive house fire can lead to a dangerous situation. In a series of apartment fire tests carried out by Aalto University, the recorded over-pressures were between 100 Pa and 1650 Pa within 50 s from the ignition [3]. They also illustrated that inward-opening doors could not be opened from inside the fire room during the over-pressure period [3]. Besides, damage in the structure caused by high pressure rise was observed in one of their fire tests. In a different context, within the PRISME (French acronym for “Fire Propagation in Elementary Multi-Room Scenarios”) fire research program, several experimental campaigns have been carried out in confined compartments, and an over-pressure up to almost 3000 Pa inside the fire room was observed [4]. Prétrel et al. [5] pointed out that the pressure peaks are an important issue for fire safety in confined and forced-ventilated enclosures. They also indicated that the pressure variation is mainly influenced by three aspects: the fire size, the ventilation conditions and the enclosure properties (thermal boundary conditions, geometry, etc.). Utiskul et al [6] studied fire behaviours under limited ventilation in a small scale compartment and observed an oscillation phenomenon of pressure inside the compartment. The experimental data, used in the present study, have been collected in a measurement campaign, performed at Umons (Belgium) [7,8].

Wahlqvist et al [9] obtained high fire-induced over-pressure in a room of tight leakage class using FDS 6.1.1. Chow et al. [10] used the Fire Dynamics Simulator (FDS) [11] version 3.01 to investigate the fire-induced pressure variation in a confined chamber and pointed out that simulation results agree reasonably well with experimental results. Beji et al [12] evaluated the capability of FDS version 5.5.3 in the simulation of a large scale, well-confined and mechanically ventilated multi-room fire scenario. Their results showed that FDS can give a good first basis for a fire hazard analysis in forced-ventilated enclosure fires provided that the HRR is known from experiments or design calculation requirements.

An over-pressure of 100 Pa in a compartment can make it impossible for people to open the inward opening doors [13]. Hence, the evacuation of occupants and rescue operations of firefighters could be hindered. On top of this, if the pressure inside a passive house reaches up to 1000 Pa, the structural integrity could be compromised. For example, in [3], a window was shattered when the internal pressure was high enough.

Although there is existing research on fire dynamics inside confined and mechanically ventilated compartments, the pressure build-up in passive houses, which could cause reverse duct flow and structural damage, has received relatively less attention. This motivates the research on fire-induced pressure variation in compartments with very low leakage area. The present work constitutes a numerical study by means of CFD, more specifically using FDS, version 6.5.2. The default settings of FDS, version 6.5.2, are used unless specified otherwise. They can be found in the user’s guide [11]. As mentioned, the experimental data from [7,8] will be used to assess the CFD results.

EXPERIMENTAL AND NUMERICAL SETUP

Geometry of the facility

There are two rooms in the experimental compartment as studied at UMons. More detail is found in [7,8], but the essential features are repeated here for the sake of ease for the reader. The floor plan of the experimental facility is shown in Fig. 1. The construction has the same inner dimensions as a 40 foot shipping container [14]. The fire source was positioned in the larger room and the two rooms are connected with a closed partition door with a small gap (90 cm^2) at its bottom. The dimensions of the fire room and the adjacent room are 7.6 m × 2.4 m × 2.4 m and 4.4 m × 2.4 m × 2.4 m respectively. An supply duct is connected to the fire room and an extraction duct is connected to the adjacent room. Thermocouple trees and pressure measurement instruments are installed in the facility, see Fig. 1.

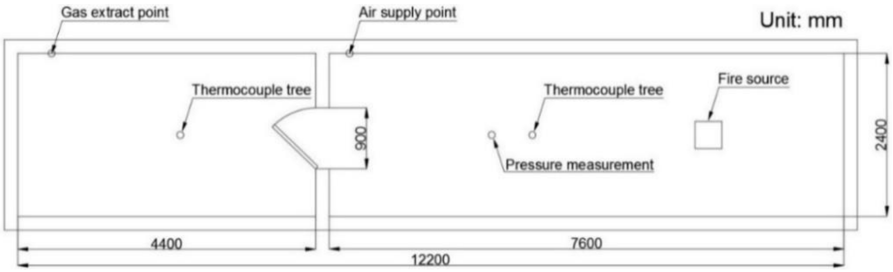

Fig. 1. Floor plan of the experimental facility.

Fire source

Overlapping wooden slats were used as a fire source in the experiment, see Fig. 2. The slats are 38 cm long and the section of a slat is 27 mm × 18 mm. There are 15 layers of slats. A stainless-steel cup 9.5 cm in diameter containing 100 ml of heptane (used for ignition) is centered below the slats.The heat release rate was calculated from the mass loss rate measured during the fire test, assuming an effective heat of combustion of 12 MJ/kg. In the simulations, the fire source was represented by a 0.4 m × 0.4 m × 0.4 m cube with prescribed HRR based on experimental results. The outputs of heat release rate in the experiments and simulations are shown in Fig. 3. For the first 60 s, there is no fire, so that the flow in the ducts can stabilize. The second peak of the heat release rate (at 560 s) was due to the collapse of the wooden slats, enhancing the combustion to some extent.

Fig. 2. Fire source in the experiments (overlapping wooden slats).

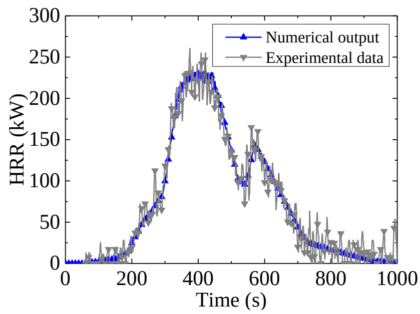

Fig. 3. Experimental and numerical heat release rate evolution in time.

Boundary conditions

The outer walls consist of three layers (from outside to inside): 0.2 m concrete, 0.05 m insulation layer and 0.026 m plasterboard. The partition wall also consists of three layers: two 0.035 m thick gypsum layers with 0.13 m rockwool in between. The partition door has two 0.004 m steel layers with 0.192 m foam in between.The thermal properties of the layers' materials are shown in Table 1. Heat transfer to the walls is calculated according to the default settings and equations in FDS.

Table 1. Thermal properties of boundary layers' materials

Material	Density (kg/m^3)	Conductivity (W/(m·K))	Specific heat (kJ/(kg·K))
Concrete	2200	0.700	0.75
Rockwool	45	0.035	0.84
Gypsum	1440	0.300	0.84
Foam	800	0.028	1.45
Steel	8050	50.200	0.49

Leakage settings

For passive houses, leakage may occur at gaps of doors, windows or wall joints. The leakage area of houses can be estimated by a fan pressurization test with a differential pressure of 50 Pa. In this work, the estimated leakage area was 0.0026 m^2. However, as explained in [15], this value arguably does not fully represent the conditions in the experiments. Indeed, fig. 4 in [15] illustrates that the leakage area from the blower door test at 50 Pa is 0.0019 m^2. A sensitivity study is considered beyond the scope of the present paper, although results have also been obtained with 0.0019 m^2 leakage area.

There are two methods to simulate leakage in FDS: Pressure Zone Leakage (Bulk Leakage) and Localized Leakage [11]. The pressure zone leakage approach is intended to capture the bulk leakage through walls. The leak flow is uniformly imposed over all surfaces that are designated as leak path. The localized leakage approach is suitable for simulating small cracks with a known location. For the pressure zone leakage approach, the volume flow rate through leakages is given by:

$$\dot{V}_L = A_L \operatorname{sign}\left(\Delta p\right)\sqrt{2\left|\Delta p\right|/\rho_\infty} \ , \qquad (1)$$

where $\dot{V}_L$ is the volume flow rate (m^3/s), A_L is the leakage area (m^2), Δp is the pressure difference between the adjacent zones (Pa) and ρ_∞ is the ambient air density (kg/m^3).

The leakage area may grow as small gaps, cracks and other leakage paths open up when the room pressure increases. In the default settings of FDS, the leakage area is assumed to be constant. In order to simulate the non-constant leakage area, FDS provides a 'LEAK_PRESSURE_EXPONENT' parameter, *n*, which can be used to reproduce the variation of the leakage area:

$$A_L = A_{L,ref}\left(\Delta p/\Delta p_{ref}\right)^{n-1/2} \ , \qquad (2)$$

where $A_{L,ref}$ is the reference leakage area (m^2) at the reference pressure difference Δp_{ref} between the adjacent zones. By default, n = 0.5, which means that the leakage area is independent of the pressure rise, and Δp_{ref} = 4 Pa. However, as the reference leakage area has been determined at a pressure difference of 50 Pa here, Δp_{ref} has been set to 50 Pa. Different values of the exponent *n* (0.5, 0.6 and 0.7) were used to study the influence of the exponent on the pressure variation which is discussed later in the present paper.

In the present work, the air leakage from the compartment to the ambient environment was simulated using the pressure zone leakage approach because the exact locations of the leakages are unknown.

The walls and ceiling were set as leak path. Since the partition door was closed during the experiment, two pressure zones (one for each room) were prescribed in FDS, in addition to the ambient pressure zone. The leakage area was evenly distributed over the walls and ceiling surface area and thus, the leakage area of the fire room and adjacent room were 0.0016 m^2 and 0.001 m^2 respectively. Furthermore, the leakage between the fire room and the adjacent room under the partition door has been prescribed using the localized leakage approach.

Ventilation system

A mechanical ventilation system was added to the compartment to study its influence on the fire behavior. In the scenario analyzed in this paper, fresh air flows into the compartment through ducts connected to the fire room while the gas was extracted from the ducts connected to the adjacent room. The lengths of the inlet duct and the outlet duct are 4.82 m and 4.11 m respectively. The diameter and roughness of the ducts are 0.1 m and 0.0015 m [14] respectively. A ventilation fan was installed in each duct with a stalling pressure of 140 Pa. The maximum duct volume flow rate was set to 80 m^3/h in the experiments, in line with Belgian requirements for residential ventilation. Two methods were used to control the volume flow rate in the simulations: by modifying the fan curve, and adding dampers. Fan curve 1 (see Fig. 4) is a simplified curve, with the maximum flow rate set to 80 m^3/h. It was used in [14] to meet the requirement of maximum duct flow rate and avoid damper modelling in the simulations. Fan curve 2 (see Fig. 4) is the actual fan curve. It interacts with dampers to meet the volume flow rate requirements. During the simulation, when reaching a point where the flow in the duct is at the maximum flow rate, the fan will not add any additional pressure and the flow rate will solely depend on the node pressures of the HVAC ductwork. If on the other hand the flow rate reaches zero, the fan will add the maximum fan pressure to the node pressure difference in the HVAC ductwork. If the pressure keeps increasing, there will be a reverse flow and the pressure rise by the fan is kept constant. It is noted that also in the experiments there was a diaphragm in the ducts and the opening percentage was about 45 %. In FDSfor a partially open diaphragm, the loss of ducts can be specified to simulate dampers that have a variable position. The effective loss of the duct, K_{eff} , can be calculated as [8, 11]:

$$K_{eff} = \left(A_{eff} / A_d\right) K_{minor} \ , \tag{3}$$

where A_{eff} is the effective area of the duct (m^2), A_d is the opening area of the diaphragm (m^2) and K_{minor} is the dimensionless "minor losses" coefficient which represents losses through components (the diaphragm here).Here, A_{eff} = 78.54 cm^2, A_d = 30.94 cm^2 and K_{minor} = 7, so the effective loss of the duct in this experiment is 17.77.

RESULTS AND DISCUSSION

Mesh sensitivity analysis

Finer mesh cell sizes allow for more resolution in simulation results, but they also consume more computational time. A mesh sensitivity analysis is performed. The required mesh cell size was first estimated using the D^* criterion [11]. The recommended ratio of $D^*/\delta x$ is between 5 and 10 [16]. In the present paper, the (cubic) mesh cell sizes, equal to 0.2 m, 0.1 m and 0.05 m, correspond to ratios equal to 2.75, 5.5 and 11, respectively. The simulation results of pressure variation and duct flow rates are shown in Fig. 5. While the D^* criterion had been developed in the context of smoke plumes, Fig. 5 illustrates that application of this criterion also leads to meshes yielding grid insensitive results for global quantities like pressure and volume flow rates. Although there are some discrepancies between 200 s and 300 s and for the peak pressure, the overall simulation results with mesh cell sizes of 0.1 m and 0.05 m are similar, while a clear difference is noted from the result with mesh cell size of 0.2 m. The relative differences of maximum pressure, inlet duct volume flow rate and outlet duct volume flow rate between 0.1 m mesh and 0.05 m mesh are 6.6%, 4.3% and 2.4%, respectively. Therefore, the mesh cell size of 0.1 m is considered fine enough for this study.

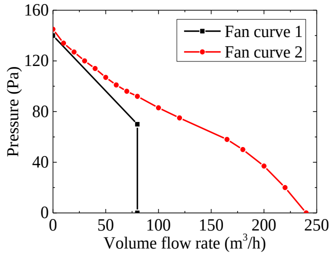

Fig. 4. Fan curves used in the simulations.

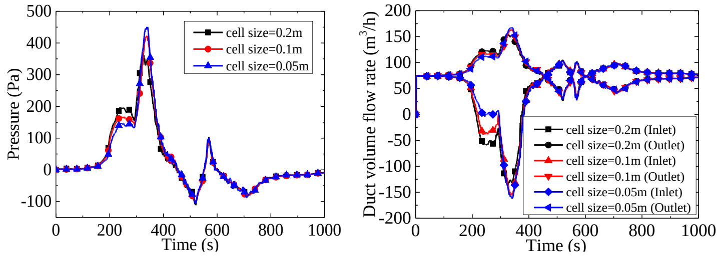

(a) (b)

Fig. 5. Simulation results using different mesh cell sizes. (a) Pressure variation in the fire room; (b) Duct flow rate. Important note: the leakage area has been set to 0.0026 m^2.

Compartment pressure variation

Simulation results using different pressure exponents and different combinations of fan curve and dampers are shown in Fig. 6. The results shown in Fig. 6 a are obtained with the combination of fan curve 2 and damper, and the results shown in Fig. 6 b are obtained with the leakage exponent n = 0.5. Previous work [17] indicates that the leakage area will increase when the pressure rises and n = 0.7 is the most suitable value when there is no ventilation system. However, the influence of the leakage pressure exponent on the pressure rise is smaller when there is a ventilation system, see Fig. **6** a. The maximum pressures obtained with different exponents are listed in Table 2. Due to the lower pressure rise compared to the configuration without ventilation, the difference between the actual pressure difference Δp and the reference pressure difference Δp_{ref} (= 50 Pa, as mentioned above), is smaller than without ventilation. This could reduce the influence of leakage pressure exponent on pressure rise. It can be seen from Table 2 that with leakage pressure exponent n = 0.5, the maximum pressure obtained is closest to the experimental value. However, it is essential to mention that this observation is only valid in combination with the value 0.0026 m^2 for leakage area. When the value 0.0019 m^2 is applied, n = 0.7 provides the maximum pressure in closest agreement with the experiments (shown in [15] and confirmed in our simulations, but not shown here). An extensive sensitivity study is beyond the scope of the present paper.

Table 2. The maximum pressure obtained with the different leakage pressure exponents. Important note: the leakage area has been set to 0.0026 m^2

Leakage pressure exponent	Maximum pressure (Pa)	Deviation from the experimental value
0.5	422.73	0.38%
0.6	383.75	8.88%
0.7	321.61	23.64%
Experiment	421.15	-

It can be seen from Fig. 6 b that when there is no damper, the resistance in the duct is much lower, resulting in more gas flowing out. Thus, the pressure rise in the compartment is underestimated. The peak value of fire-induced over-pressure in the fire room is about 420 Pa. The inclusion of the damper in the simulations is essential to reach the maximum pressure level as measured. During the decay period, an under-pressure of about -140 Pa is observed due to the cooling down of gases in the compartment. The reduction in pressure seems exaggerated in the simulations during the first part of the decay period. As a consequence, the second pressure peak, due to the second peak in HRR (see Fig. 3), is under-predicted, although the pressure difference between the first minimum (at t = 549 s) and the second maximum (at t = 578 s), is well captured (230.87 Pa in the experiment, vs. 200.22 Pa in the simulations). The decay in pressure during the second part of the decay period in HRR is less pronounced in the simulations.

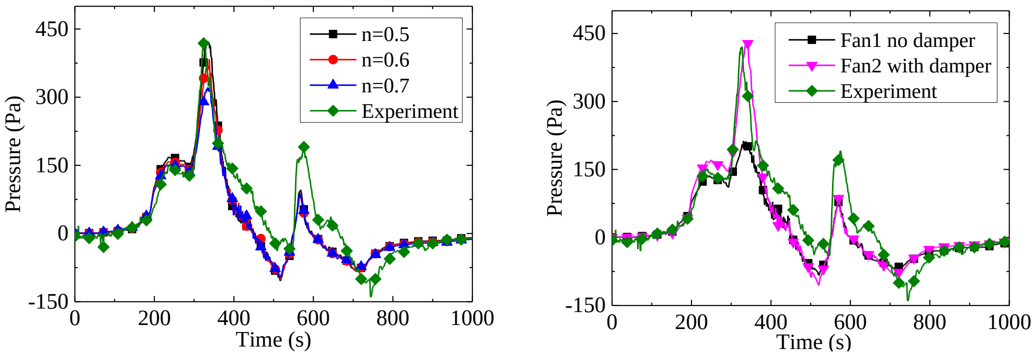

(a) (b)

Fig. 6. Pressure variation as function of time in fire room. (a) For different pressure exponents (fan curve 2, with damper); (b) For different combinations of fan curves and dampers (n = 0.5). Important note: the leakage area has been set to 0.0026 m^2.

Ventilation duct flow

The duct flow rates are shown in Fig. 7. During the first 60 s, the flow in the duct reaches a steady state. The volume flow rates generated by fan curve 1 without damper and fan curve 2 with damper both meet the requirement of 80 m^3/h. As such, the 2 mentioned combinations are a good representation of reality prior to the fire. The combination of fan curve 2 and damper also resembles the experimental set-up in reality better. When the room pressure exceeds the stalling pressure of the ventilation fan (see Fig. 4), it causes reverse flow in the inlet duct, causing smoke spread into the inlet duct. As mentioned above, the reverse flow solely depends on the pressure difference between nodes. The configuration of fan curve 1 without damper has a smaller pressure difference and lower duct resistance while the configuration of fan curve 2 with damper has higher pressure difference and higher duct resistance. This results in the similar reverse flow in the simulations. In the period 220 s – 300 s, differences are visible, though Fig. 6 b reveals that with fan 2, with damper, the pressure rise inside the compartment just exceeds the stalling pressure, while this does not happen with fan 1. The reason is the much lower resistance in the outlet duct (no damper). As for the outlet flow, the configuration of fan curve 1 without damper exceeds the maximum flow rate of the fan, so the fan does not affect the duct flow. With fan 2 with damper, the flow rate does not exceed the maximum flow rate, so the fan still has influence on the duct flow. The maximum measured reversed volume flow rate, occurring at approximately 330 s from the beginning of the experiment, is 137 m^3/h (Fig. 7 a). On the contrary, the volume flow rate in the outlet duct increases due to the pressure rise inside the enclosure, up to 175 m^3/h (Fig. 7 b). It can be seen from Fig. 7 that the combination of fan curve 2 and dampers is better in line with experimental results. This indicates that the simplified fan curve cannot reproduce the experimental results effectively. All elements in the experiment should be set to gain reasonable simulation results, particularly with respect to pressure peaks.

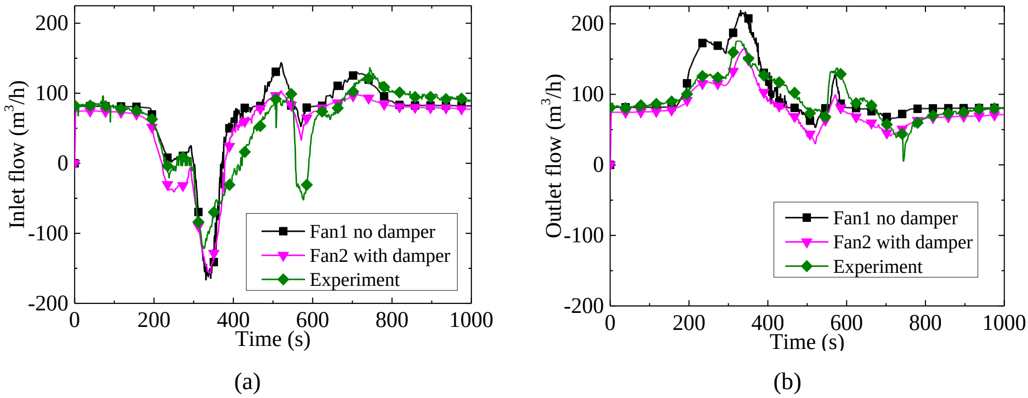

Fig. 7. Evolution of volume flow rate with time. (a) Inlet duct; (b) Outlet duct. Important note: the leakage area has been set to 0.0026 m^2.

Pressure difference between rooms

The pressure variation inside the adjacent room for the configuration of fan curve 2 with damper is shown in Fig. 8 a. In order to reduce the pressure rise in the adjacent room, the gap area between rooms can be reduced. Simulating the fire scenarios with 1/2, 1/5 and 1/10 of the original gap area between rooms, i.e., reducing the gap area from 90 cm^2 to 9 cm^2, the pressure rise in adjacent room reduces significantly (Fig. 8 a and Fig. 9). For the gap areas of 18 cm^2 and 9 cm^2, the adjacent room is even in a negative pressure state during the initial stage because the amount of air extracted through the outlet duct exceeds that leaked from the fire room. Figure 9 shows how the maximum pressure difference between the fire room and the adjacent room decreases as the gap area increases. The maximum pressure difference between the rooms has a 20-fold increase for a 10-fold reduction in gap area (from 90 cm^2 to 9 cm^2). Therefore, reducing the gap area between rooms might significantly decrease the pressure rise in the adjacent room, thereby reducing the associated risk with respect to opening doors in the adjacent room. It is worth noting, though, that the reduction of gap area will also result in higher pressure rise in the fire room, see Fig. 8 b. The maximum pressure in the fire room increases from 420 Pa to 930 Pa as the gap area reduces from 90 cm^2 to 9 cm^2.

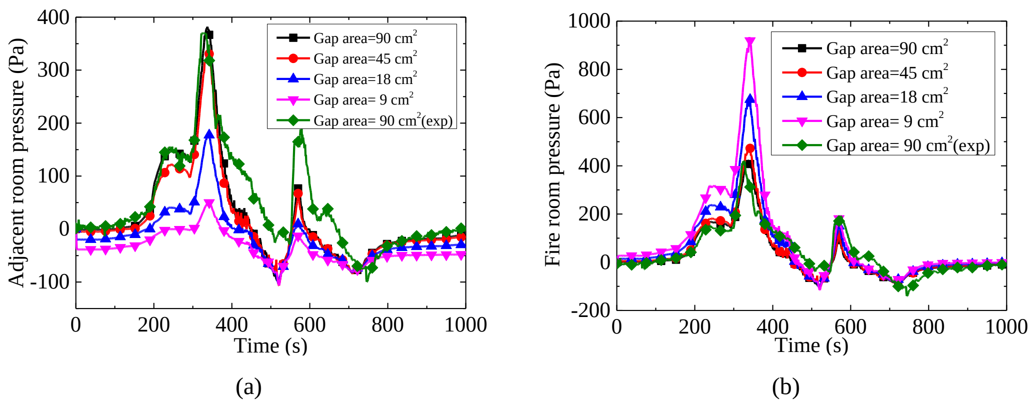

Fig. 8. Pressure variation as function of time for different gap areas. (a) Adjacent room; (b) Fire room. Important note: the leakage area has been set to 0.0026 m^2.

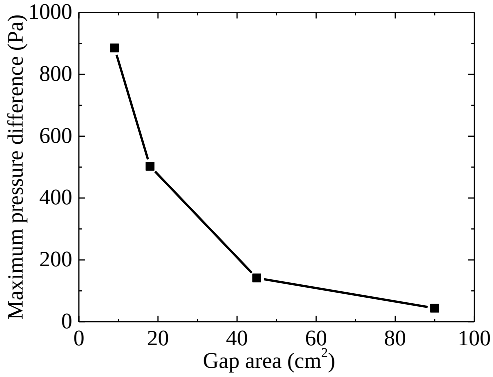

Fig. 9. Maximum pressure difference as function of gap area between fire room and adjacent room. Important note: the leakage area has been set to 0.0026 m^2.

CONCLUSIONS

The present study focuses on the fire-induced pressure variation in an experimental 2-room set-up, resembling settings of passive houses. Mechanical ventilation is in place for the well-confined rooms and there is reverse flow in the supply duct due to the fire-induced pressure rise. The measured fire-induced pressure rise in the fire room reached up to 420 Pa, which is high enough to impede occupant's evacuation and firefighter's rescue operation. The high pressure inside the confined compartment caused a 137 m^3/h reverse flow in the supply duct, while it increased the flow in the extraction duct up to 175 m^3/h.

A mesh sensitivity study suggested that the mesh cell size of 0.1 m is sufficient for the CFD simulations of the compartment fire at hand.

The influence of the leakage pressure exponent on the maximum fire-induced pressure rise in the simulations, with, as expected, a lower maximum pressure rise if gaps are expanding as the pressure rises (i.e., $n > 0.5$). The impact is smaller than in previous work [17], where there was no mechanical ventilation system. The value $n = 0.5$ seems optimum for the present study, but this observation only valid in combination with the value 0.0026 m^2 for leakage area. When the value 0.0019 m^2 is applied, $n = 0.7$ provides the maximum pressure in closest agreement with the experiments [15].

It is important to include the dampers, present in the experimental set-up, in the simulations in order to obtain good agreement for the temporal evolution of pressure inside the compartment. Replacing their effect through a modified fan curve is not sufficient.

The recorded pressure rise in the adjacent room also reached a dangerous level in the experiments. Reducing the gap area between the rooms reduces the pressure rise in the adjacent room but causes even higher pressure levels in the fire room.

ACKNOWLEDGMENTS

The authors would like to thank the China Scholarship Council (CSC) for the financial support of the first author (Grant No. 201706420076), as well as the co-funding from Ghent University through BOF (Grant No. 01SC2018).

REFERENCES

[1] I. Sartori, A.G. Hestnes, Energy Use in the Life Cycle of Conventional and Low-energy Buildings: A Review Article, Energy and Buildings. 39 (2007) 249-257.

[2] S. Brohez, P. Duhamel, Inwards Doors Blocked by Fire Induced Overpressure in Airtight Apartment: a Real Case in Germany, Chemical Engineering Transactions. 67 (2018) 25-30.

[3] R.K. Janardhan, S. Hostikka, Experiments and Numerical Simulations of Pressure Effects in Apartment Fires, Fire Technology. 53(2017) 1353-1377.

[4] L. Audouin, L. Rigollet, H. Prétrel, W. Le Saux, M. Röwekamp, OECD PRISME Project: Fires in Confined and Ventilated Nuclear-type Multi-compartments-Overview and Main Experimental Results, Fire Safety Journal. 62(2013) 80-101.

[5] H. Prétrel, W. Le Saux, L. Audouin, Pressure Variations Induced by a Pool Fire in a Well-confined and Force-ventilated Compartment, Fire Safety Journal. 52(2012) 11-24.

[6] Y. Utiskul, J.G. Quintiere, A.S. Rangwala, B.A. Ringwelski, K. Wakatsuki, T. Naruse, Compartment Fire Phenomena Under Limited Ventilation, Fire Safety Journal. 40(2005) 367-390.

[7] S. Brohez and I. Caravita, Overpressure induced by fire in airtight buildings, Journal of Physics: Conference Series. 1107 (2018).

[8] I. Caravita, Fire Development in Passive Houses: Experimental Analysis and Validation of Theoretical Models, Master thesis, Università di Bologna, Bologna, Italy, 2017.

[9] J. Wahlqvist, P. van Hees, Evaluating Methods for Preventing Smoke Spread through Ventilation Systems Using Fire Dynamics Simulator, Fire and Materials. 41(2017) 625-645.

[10] W.K. Chow, G.W. Zou, Numerical Simulation of Pressure Changes in Closed Chamber Fires, Building and Environment. 44(2009) 1261-1275.

[11] K. McGrattan, S. Hostikka, R. McDermott, J. Floyd, C. Weinschenk, K. Overholt, Fire Dynamics Simulator, User's Guide, NIST special publication 1019, sixth ed., Gaithersburg and Espoo, 2013.

[12] T. Beji, F. Bonte, B. Merci, Numerical Simulations of a Mechanically-Ventilated Multi-Compartment Fire, In: D. Nilsson, P. van Hees, R. Jansson (Ed.), Fire Safety Science–Proceedings of the Eleventh International Symposium, pp, 499–509, 2014.

[13] S. Hostikka, R.K. Janardhan, U. Riaz, T. Sikanen, Fire-induced Pressure and Smoke Spreading in Mechanically Ventilated Buildings with Air-tight Envelopes, Fire Safety Journal. 91(2017) 380-388.

[14] D. C. O. Cruz, Numerical Simulations of Pressure Effects in the Event of Fire in Passive Houses, Master thesis, Ghent University, Ghent, Belgium, 2018.

[15] S. Brohez and I. Caravita, Fire induced pressure in passive houses: Experiments and FDS validation, 9th International Seminar on Fire and Explostion Hazards, St-Petersburg (2019).

[16] K. McGrattan, Verification and Validation of Selected Fire Models for Nuclear Power Plant Applications Volume 7: Fire Dynamics Simulator, Report No. NUREG-1824, U.S. Nuclear Regulatory Commission., 2007.

[17] J. Li, T. Beji, B. Merci, Preliminary Numerical Study of Fire-Induced Pressure Rise in a Passive House Compartment, Journal of Physics: Conference Series. 1107(2018) 042026.